TECTONIC DEFORMATION OF A LACUSTRINE MUDSTONE AT SODA LAKE GEOTHERMAL FIELD, WESTERN NEVADA, USA, FROM 3D SEISMIC INTERPRETATION

T. Kent[1,2], and J. N. Louie[1] (Presenter)

[1]Nevada Seismological Laboratory MS 0174, University of Nevada, Reno, Nevada, USA

[2]now at: Noble Energy Inc., Denver, Colorado, USA

louie@seismo.unr.edu

Keywords: *3D Seismic, Tectonics, Geothermal, Walker Lane.*

ABSTRACT

The transition between the two structural and fault regimes of the right-lateral Walker Lane and the extensional Basin and Range, Nevada, allows for complex transtensional fault interactions. This study investigates this tectonic shift in the Carson Sink using the fault offsets of a paleo-planar lacustrine mudstone in a 3D seismic-reflection data volume at the Soda Lake Geothermal Field. The 3D and three-component reflection seismic survey covers an area of 34 sq km with 8374 source points and 3001 receivers. A Recent sandstone/mudstone package is a strong and the most expansive reflector in this survey, appearing from 0.2 to 0.3 seconds, at an approximate depth of 240 m. The interpreted mudstone reflectors illuminate a fault map of recent active tectonics in this basin. Fault offsets of this unit demonstrate post-depositional structural deformation of the Soda Lake geothermal field. Using OpendTect® allowed multiple steps in specialized workflows to facilitate the interpretation of faults and horizons in this seismic-reflection data volume. A dip-steered, median-filtered, and diffusion-filtered volume gave sharper contrasts at the faults. Using this fault-enhanced data volume assisted the interpretation of the surface of the mudstone horizon and the faults that offset reflectors above and below the unit. The fault patterns show en echelon fault steps, large left bends and some antithetic-striking faults. Total horizontal offset across all the faults is 96 m across 5.4 km, yielding 1.8% as a value for recent extensional strain across the survey. The horizon map of the mudstone has a relative low point in the accommodation zone that accompanies a left bending fault and coincides with the most productive part of the geothermal field. A structural ramp between the major faults on the west side suggests a structural interpretation as a normal-fault step-over zone, supposing a lack of strike-slip motion or pull-apart mechanics.

1. INTRODUCTION

1.1 Geologic and Tectonic Setting

The movement along the North American-Pacific plate boundary is unevenly distributed, with approximately half of the deformation being accommodated on the San Andreas fault, but variable depending on the latitude (e.g., greater percentage of motion is accommodated in northern California on the San Andreas fault than in southern California; Wesnousky, 2005b). Dextral shear also occurs along the Walker Lane Deformation Belt and Eastern California Shear Zone (Wernicke, 1992; Atwater and Stock, 1998). This transition zone of the Walker Lane is allowing the northward movement of the Sierran Microplate (Figure 1) relative to the Basin and Range Province (Stewart, 1988). According to GPS geodetic studies 20-25% of the plate motion occurs along the Walker Lane in the form of transtensional deformation (Bennet et al., 1998; Faulds et al. 2005; Wesnousky, 2005b; Hammond et al., 2011).

The Northern Walker Lane (NWL) accommodates transtension along the transition of the Basin and Range Province and the Sierra Nevada/Great Valley Microplate on overlapping, left-stepping dextral faults that are being modified due to a young dynamic change in the stress regime (Unruh et al., 2003). One of the sources of this change is from northward migration of the Mendocino triple junction (Faulds et al., 2005). These dextral faults tend to transition to more normal offset and northern strike as they exit the shear of the NWL and enter the extension of the Basin and Range (Faulds et al., 2005; Wesnousky, 2005a; Wesnousky et al., 2012). Left stepping dextral faults should enable clockwise rotations of fault blocks. But, the majority of fault block rotation in GPS is seen to be slightly counter-clockwise for the NWL (Hammond et al., 2011). Macroscopic Riedel shears are employed as a hypothesis that these stepping-faults are migrating toward the maximum extension in a counter-clockwise development that could account for the GPS block rotation observed (Faulds et al., 2005).

1.2 Carson Sink

The Carson Sink trends NE like much of the Basin and Range topography, although it has a more equant shape (Figure 1). The basin is overlain by Quaternary alluvium, sand dunes, silt and a large playa surface (McNitt, 1990). Like many of the basins in Western Nevada, the Carson Sink exhibits lacustrine deposits that can be attributed to Pleistocene Lake Lahontan (Adams and Wesnousky, 1999; Benson et al., 2002). The NWL tectonic belt borders this area toward the west. Surface faulting indicates basin bounding normal faults (Bell, 1984) and some evidence of strike-slip faulting in the basin (dePolo, 1998; Caskey et al., 2004). The Carson Sink is the surface expression of a complex interaction of shear and extensional forces that cause crustal block rotation (Faulds and Perkins, 2007). It has been proposed that the transfer of NW-trending dextral shear in the Walker Lane to WNW extension in the northern Great Basin would allow for the formation of enhanced extension and pull-apart basins that bring about structural controls for geothermal systems (Faulds and Henry, 2008).

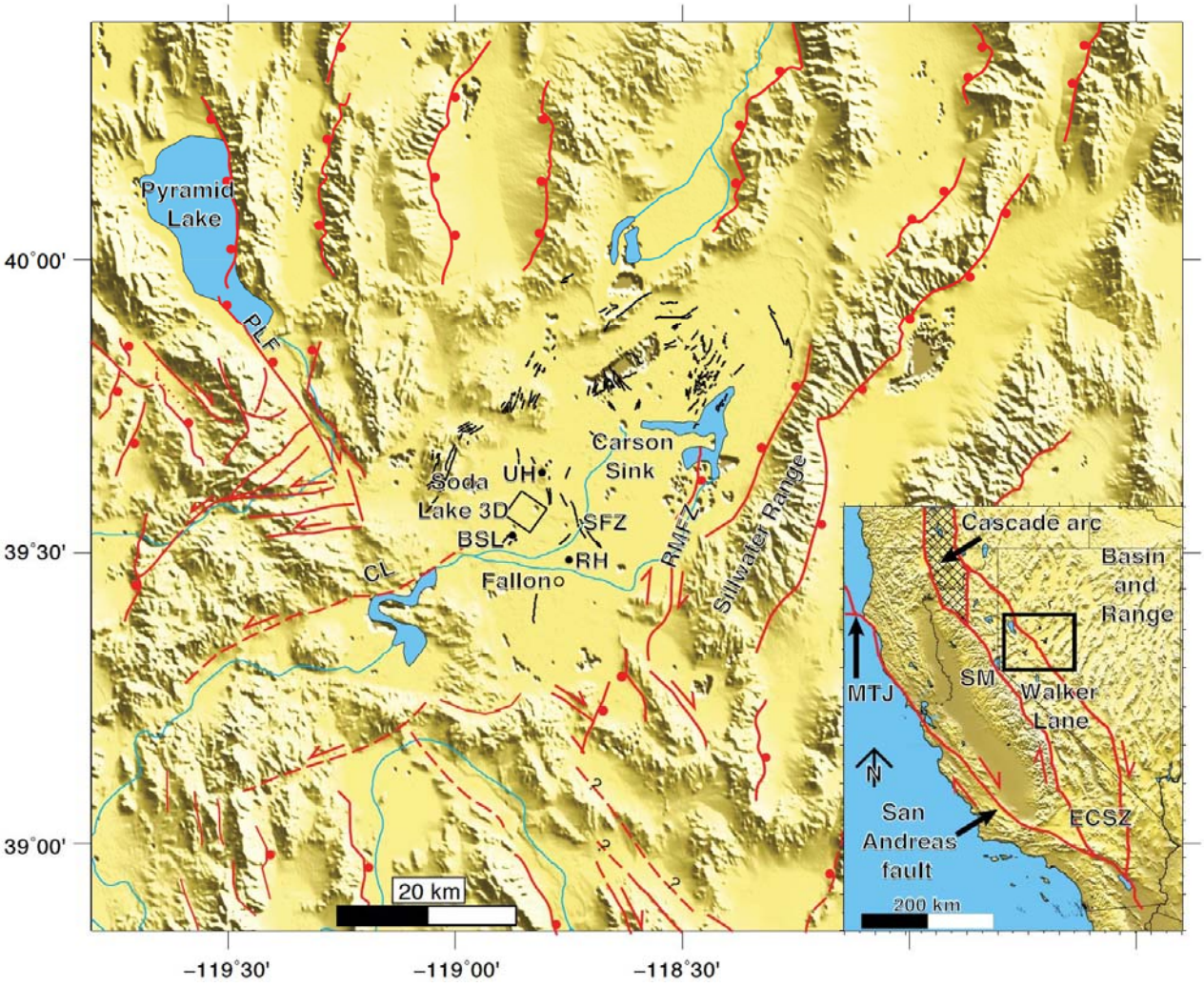

Figure 1: Study area in western Nevada, including major structural trends simplified in red with mapped faults in the Carson Sink in black. Black box indicates the area of the Soda Lake 3D seismic survey. *PLF* - Pyramid Lake fault; *CL* – Carson lineament; *SFZ* - Sagouse fault zone; *RMFZ* - Rainbow Mountain fault zone; *UH* - Upsal Hogback; *BSL* - Big Soda Lake; *MTJ* - Mendocino triple junction; *ECSZ* - Eastern California shear zone; *SM* - Sierran Microplate; *RH* - Rattlesnake Hill. Modified from U.S.G.S. (2006); Faulds et al. (2005); Caskey et al. (2004); Eisses (2012).

1.3 Soda Lake Geothermal Field

The Soda Lake geothermal field is located 10 km (6 mi) northwest of the town of Fallon in Churchill County, Nevada (Figure 1). It is in the south-central part of the Carson Sink, which is bordered by the <10,000 year-old Big Soda Lake volcanic explosion crater to the south, and the 25,000 year-old mafic Quaternary Upsal Hogback volcanic complex to the north (Hill et al., 1979; Sibbett, 1979; Cousens et al., 2012). There are multiple operating geothermal fields within 50 km (30 mi) of Soda Lake (McLachlan et al., 2011).

There are two current power plants, Soda Lake 1 (5.1 MW gross) and Soda Lake 2 (18 MW gross), although they have never reached maximum output. Twenty three large diameter wells and six re-drills have been completed, with five used for production and five for injection. This low success rate is due to an inadequate model of the resource, with drilling sites located near the central part of a shallow thermal anomaly (Echols et al., 2011).

The geothermal field was chosen for an American Recovery and Reinvestment Act (ARRA) award for the U.S. Dept. of Energy Validation of Innovative Exploration Technologies in the Geothermal Technologies Program. This provided the funding for the 3D seismic study (Gundy et al., 2010). While most geothermal lithologies in primarily volcanic regions are lacking in clean reflections, this site had a four-line seismic survey done by Chevron in the 1970's that imaged coherent reflections (Echols et al., 2011). These horizontal and expansive reflections of thick sand and mudstone stratigraphy, relatively anomalous in Nevada geothermal systems, made this 3D survey viable at Soda Lake (Echols et al., 2011). At 34 sq km of seismic data, this is one of the largest seismic surveys of any geothermal field to date.

The seismic volume yielded a detailed map of the fault deformation of the same mudstone horizon found by Chevron, and also defined an inverted-cone-shaped basaltic unit at about 550 m depth (Echols et al., 2011). This extrusive basaltic unit has been dated to about 5.1 Ma (McLachlan and Faulds, 2012). The structural style of this

field was interpreted by the operating company to be one of nested pull-apart basins with the thickest sections of basalt in the center of the production area (Echols et al., 2011). Some of the larger fault picks lined up with higher thermal anomalies in wireline data (J. Echols, pers. comm.).

1.4 Mudstone Reflector

A sandstone/mudstone package is the strongest reflector in this survey, appearing from 0.2 to 0.3 seconds two-way travel time, at an approximate depth of 240 m. The interpreted mudstone reflectors illuminate a fault map of recent active tectonics in this basin. This reflective unit consists of shale, mudstone and fine sand that formed in a deep lacustrine environment (Sibbett, 1979). Assuming an environment of deep lake sediments, this unit was deposited in a paleoplanar orientation. Therefore fault offsets of this unit should demonstrate post-depositional structural deformation of the Soda Lake geothermal field (Echols et al., 2011).

The periodic presence of Lake Lahontan is common in Western Nevada basins for the last 1 Ma, including Carson Sink, Pyramid Lake to the northwest and Walker Lake to the southwest (Reheis, 1999). Pyramid Lake shows Pleistocene sedimentation rates from sediment cores, which indicate that between 47.9 ka and 13.9 ka there was 17.32 m of sediment deposition, giving a Pleistocene rate of 0.51 mm/yr (Eisses, 2012).

These Pyramid Lake sediment layers are continuous and show consistent deposition of these reflective units for tens of meters of thickness (on the order of >100 ka) past the oldest dates in seismic CHIRP imagery (Eisses, 2012). Walker Lake shows higher sedimentation, of 10 m from 13-21 ka, yielding a rate of 1.25 mm/yr (Benson, 1988). These rates are likely overestimations when applied to the more cyclic nature of deposition in the Carson Sink, and are used as minimums.

The Rattlesnake Hill basalt, at depth, is about 5 km southeast of the 3D seismic survey (Figure 1). This volcanic cone was likely erupted subaerially on the paleosurface of the Carson Sink and ranges in age from 2.5 to 1.03 Ma (Maurer and Welch, 2001). The closest basalt age to Soda Lake that is on the lateral extent of the basalt flow is 1.5 Ma and is 30 m below the shallowest indication of the mudstone reflector. Assuming a simple layer cake model for lacustrine sediments, this indicates a maximum age for the mudstone around 1.5 Ma.

1.5 3D Seismic Survey

The 3D (and three-component) reflection seismic survey occupies an area of 34 sq km with 8,374 source points and 3001 receivers. There are 52 paired source lines with a pair separation of 33.5 m. Source interval is 33.5 m and the paired, northeast-trending source lines are separated by 235 m. Receivers are spaced at 67 m on 36 northwest-trending lines separated by 168 m. This design provides 17 m common midpoint (CMP) bins with high fold (40) in the 600 by 1200 meter-deep area of the geothermal reservoir. The mudstone under investigation here is shallower and therefore potentially has lower seismic fold. This geometry was originally planned for just single component geophones, but during project approval it was upgraded to include three-component recording. Due to the long permitting process already underway the geometry of the survey could not be changed. The source is alternating sets of three 28,000 kg vibrator trucks producing two sixteen-second-long, 8-72 Hz sweeps per source point.

This survey's P-wave data were processed first with a field static correction, and then a model-based noise attenuation to eliminate low-velocity surface-wave noise. Two passes of stacking velocity analysis with a 0.8 km interval and surface-consistent residual statics were done. A curved-ray 3D Kirchhoff prestack time migration (PSTM) provided velocity analysis. Another curved-ray 3D Kirchhoff PSTM approach with sufficient half-aperture, 75-degree migration dip, including P-wave VTI-anisotropy (if significant) and PSTM residual velocity analysis, yielded the final image volume. The velocity model applied to convert the PSTM to prestack depth migration (PSDM) is relatively simple and horizontally continuous for the shallow section at and above the mudstone, although it accounts for the faster velocities and lateral heterogeneity at the basaltic unit (Echols et al., 2011).

We interpreted the seismic volume in OpendTect®. Multiple steps were taken according to specialized workflows to facilitate the interpretation of faults and horizons in this volume. First, a dip-steered volume was produced to allow for the following processing of attributes to steer according to the structural dip of the reflections. A median filter applied to the volume reduced noise spikes and preserved reflection trends. Similarity attributes calculated located reflection offset in the volume to get a non-interpreted fault map along the Z-plane (Chopra and Marfurt, 2007). To give a sharper contrast at the faults, reflector amplitudes were migrated toward areas of lower similarity using a diffusion filter (Figure 2). Using this fault-enhanced volume assisted the interpretation of the surface of the mudstone horizon and the faults that offset reflectors above and below the unit.

2. DATA ANALYSIS

Faults and horizons picked in the 3d seismic provide interpreted structural offsets of the paleoplanar mudstone in the seismic volume. To facilitate the picking of faults the “similarity” seismic attribute volume in horizontal, constant-depth section recognizes the recent fault pattern cutting the mudstone (figure 2). This map view shows the general strike of the faults and the nature of their discontinuities.

The majority of picked fault planes strike between north and northeast with some antithetic faults in the central part of the survey (figure 3). The fault patterns show en-echelon fault steps, large left bends and some antithetic-striking faults.

Fault picks were made on the inline vertical sections of the fault-enhanced seismic volume because it is closer to perpendicular to the general fault strike. The fault picks were then checked on the crossline vertical sections. The faults are assumed to be planar and have normal displacement. A minimum of 6 m of vertical offset in the mudstone is nominally required to delineate any fault because 6 m is a quarter of the wavelength of the dominant frequency (~70 Hz) of the mudstone reflector. The best-picked faults cut both deeper features, and the mudstone by more than 6 m (e.g., #1 in figure 4). Less well-observed faults cut the mudstone but less clearly offset the lower stratigraphy (#2 in figure 4). Faults that offset both the mudstone and lower units are picked until all units are continuous again. This can result in fault picks that have little to no mudstone offset in certain cross-sections (#3 in Figure 4). Often in this survey the lower units have larger offset along the fault plane than the mudstone. There are

also discontinuities that are artifacts of the fault enhancement process that are not picked as faults (#4 in Figure 4).

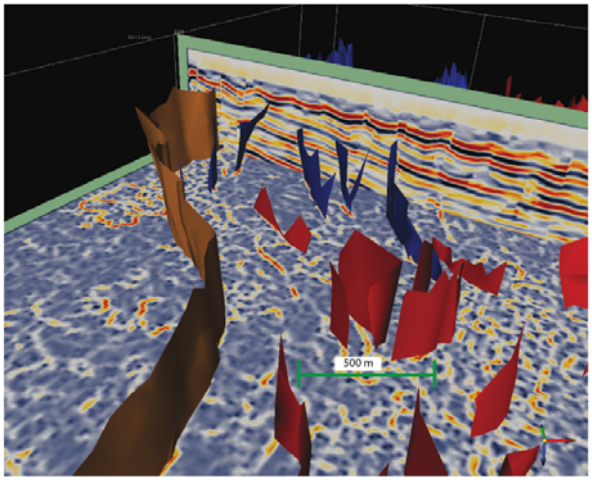

Figure 2: Picked fault planes sticking out of a z-plane that shows zones of lower similarity along fault planes. Not all of the low-similarity lines have faults, because they may not have been continuous enough to offset the shallower mudstone. The cross section shows the fault-enhanced seismic volume. Vertical exaggeration is 5 times.

To analyze the dip direction of the faults a simplified fault map is prepared, to estimate the strike of over one hundred faults. The calculation of the extensional direction involves the assumption that all north to northeast striking faults have an eastern dip. This avoids the bimodal distribution of the same extension directions from horst and graben features that have parallel strikes but oppositely dipping fault planes. The rose diagram shows a mean fault dip trending 102º.

The vertical offset and dip of the faults are calculated along a cross section located perpendicular to faulting (Figure 4). There are 13 faults across this line with 8 dipping east and 5 dipping west. The average dip of these faults is 66º with a total length of the cross section being 5.4 km. If the horizontal offset of all the faults is individually totaled, the offset is calculated at 96 m across 5.4 km. Assuming that this is a paleoplanar lacustrine mudstone then we can use this as a value for extension across the survey, a cumulative extensional strain of 1.8%.

The mudstone unit is expressed as a source waveform of large amplitude in the clearest areas of the seismic survey (Figure 4). The choice to tie the mudstone horizon to the first maximum positive seismic amplitude reflection arises from the overall coherence of that feature throughout the survey area. In some areas this maximum positive becomes the only high-amplitude reflection to follow (#5 in Figure 4). The gamma ray logs in four wells also indicated that this reflector had the broadest peak in radioactivity, indicating a more consistent and thicker fine-grained lithology. Using the well logs and cores to tie this horizon to depth, the deformation in this unit can yield direct evidence of strain during the Pleistocene or possibly even the Pliocene, depending on the uncertain age of this unit, perhaps somewhere between the extremes of 0.5 to 1.5 Ma.

Topography of the mudstone unit shows a relative low near the bend of the faults that coincides with where peak geothermal production is located (Figure 3). Along the east side of the survey there is an interpreted horst or half-graben structural feature that creates a ridge in the mudstone horizon striking north-south.

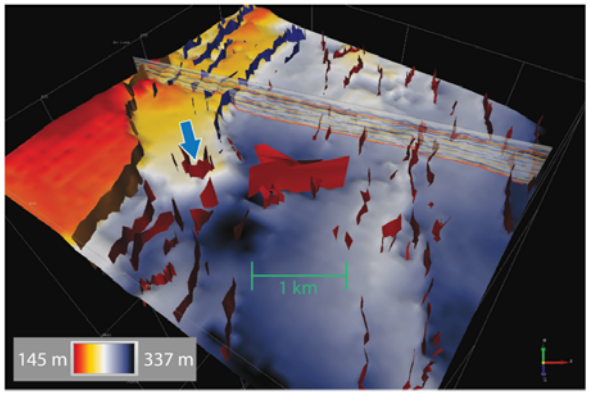

Figure 3: An oblique view of the mudstone horizon topography with fault picks shown. The geothermal production and relative mudstone low is south of the east-striking faults. The structural ramp is shown on the west side of the image sloping down toward the viewer from a red high to a blue low. The relative ridge is along the east side. Semi-transparent cross-section is the same as Figure 4. The arrow indicates the ramp, between two major faults, that leads toward the highly faulted accommodation zone. Color on the fault planes is used just to differentiate zones of faulting across the field. Color bar indicates depth to mudstone. Vertical exaggeration is 5 times.

There is a ramp between the two major faults on the west side of the study that slopes down to the south. The horizon is at a mean depth of 255 m and a minimum of 150 m.

3. INTERPRETATION

The temporal setting of the paleoplanar mudstone is uncertain. The extrusive basalt at 600 m depth provides an absolute maximum age of 5.1 Ma and the basalt at Rattlesnake Hill provides a more reasonable maximum age of 1.5 Ma. Assuming a sedimentation rate similar to Pyramid Lake at 0.51 mm/yr (Eisses, 2012), the mean depth to the mudstone horizon (255 m) would indicate an age of 500 ka. If the minimum depth (150 m) is used this would yield an age of 294 ka. Using the minimum depth does not factor in preferential deposition into relative topographical lows. Assuming that the mean depth yields a minimum age of the mudstone, the extension of 96 m gives a maximum extension rate of 0.19 mm/yr. This rate would be even higher if the age of 294 ka was used. Using the inferred maximum age (1.5 Ma) of the mudstone, the rate is 0.064 mm/yr. A rate of 0.19 mm/yr is almost a fifth of the extension along a nearby GPS profile extending 250 km across the Basin and Range (Hammond et al., 2011), all in just 5.4 km. The minimum rate of 0.064/yr is still three times larger (for 5.4 km) than the average Basin and Range strain in the same GPS profile. This seems unreasonable; either this age is far too young or extension related to the NWL is enhancing this estimate near the Soda Lake 3D survey area.

The structural map from the depth of the mudstone horizon (Figure 3) shows a ramp leading to a relative low point.

With no piercing point, there is no way to infer the amount of strike slip motion for these faults. The 3D seismic shows good evidence for pure extension in the localized area of the geothermal field, and if the system was purely extensional, it would be interpreted as a step-over or relay ramp in a normal fault zone (Larsen, 1988; Faulds et al., 2005), although the 3D seismic survey lacks a major fault to carry the offset to the south (Figure 4).

A pull-apart basin is another interpretation that would allow for partitioning of normal and strike-slip motion (Wu et al. 2009; Brothers et al., 2009; Gürbüz, 2010; Mann et al., 1983). This model would account for the consistent east-dipping faults and the step-over with pure extensional displacement in the Soda Lake 3D. For this hypothesis to be valid there also needs to be dextral-slip motion orientated 120º from the extensional faults. This dextral motion would be striking 134º compared to the 14º strike of the mean fault direction in the study. This orientation coincides with NWL tectonics surficially shown by faults along the southern boundary of the Carson Sink and the Sagouse fault zone to the northeast of the seismic study (Figure 1). However there is no NWL-oriented fault to the northwest of the 3D seismic to connect possible strike-slip offset. Pull-apart basins also tend to focus extension (Wu et al., 2009), which could account for the specific points of recent volcanism expressed on the surface by Big Soda Lake and the Upsal Hogback.

4. CONCLUSION

Using 3D seismic we produce a representation of the deformation in the Carson Sink, Nevada that allows for multiple structural hypotheses to explain localized extension and crustal thinning. A fault and horizon map of the Soda Lake 3D is produced and quantified to indicate that this system is undergoing higher deformation than expected from the surrounding slow Basin and Range tectonics. The seismic volume demonstrates evidence for comparatively large amounts of offset, in comparison to Basin and Range expectations, indicating some influence from the Northern Walker Lane. The two interpretations of either a step-over or pull-apart system are presented and there is not yet slip evidence to disprove either.

ACKNOWLEDGEMENTS

The authors would like to thank Magma Energy (U.S.) Corporation for their cooperation in providing the data and support, Dawson Geophysical Company for conducting the survey, and Geokinetics for data processing. The 3D seismic volume manipulation and visualization was performed in OpendTect®. Magma Energy received support for this project from the American Recovery and Reinvestment Act (ARRA) through the US Dept. of Energy Geothermal Technologies Program. Kent was supported in part by the Great Basin Center for Geothermal Energy through funding from the Department of Energy.

REFERENCES

Adams, K. D., and S. G. Wesnousky, 1999, The Lake Lahontan highstand: age, surficial characteristics, soil development, and regional shoreline correlation: Geomorphology, 30, 357-392.

Atwater, T., and J. Stock, 1998, Pacific-North America plate tectonics of the Neogene Southwestern United States: An update: International Geology Review, 40.

Bell, J. W., 1984, Quaternary fault map of Nevada, Reno: Scale 1:250,000, Nevada Bureau of Mines and Geology Map 79.

Bennet, R. A., B. Wernicke, and J. Davis, 1998, Continuous gps measurements of contemporary deformation across the northern Basin-Range province: Geophysical Research Letters, 25, 563-566.

Benson, L., 1988, Preliminary paleolimnologic data for the Walker Lake subbasin, California and Nevada: Water-Resources Investigations Report 87-4258, U.S. Geological Survey.

Benson, L., M. Kashgarian, R. Rye, S. Lund, F. Paillet, J. Smoot, C. Kester, S. Mensing, D. Meko, and S. Lindstrom, 2002, Holocene multidecadal and multicentennial droughts affecting northern California and Nevada: Quaternary Science Reviews, 21, 659-682.

Brothers, D. S., N. Driscoll, G. M. Kent, A. J. Harding, J. M. Babcock, and R. L. Baskin, 2009, Tectonic evolution of the Salton Sea inferred from seismic reflection data: Nature Geoscience, 2, 581-584.

Caskey, S. J., J. W. Bell, A. R. Ramelli, and S. G. Wesnousky, 2004, Historic surface faulting and paleoseismicity in the area of the 1954 Rainbow Mountain-Stillwater earthquake sequence, central Nevada: Bulletin of the Seismological Society of America, 94, 1255-1275.

Chopra, S., and K. Marfurt, 2007, Seismic attributes for prospect identification and reservoir characterization: Society of Exploration Geophysicists. SEG Geophysical Developments Series, No. 11.

Cousens, B., C. D. Henry, and V. Gupta, 2012, Distinct mantle sources for Pliocene-Quaternary volcanism beneath the modern Sierra Nevada and adjacent Great Basin, northern California and western Nevada, USA: Geosphere, 8, 562-580.

dePolo, C., 1998, A reconnaissance technique for estimating the slip rate of normalslip faults in the Great Basin, and application to faults in Nevada, U.S.A. University of Nevada, Reno unpublished Ph.D. dissertation.

Echols, J., D. Benoit, M. Ohren, G. Oppliger, and T. V. Gundy, 2011, Integration of a 3d-3c reflection seismic survey over a known geothermal resource: Soda Lake, Churchill County, Nevada: Transactions, Geothermal Resources Council, 1633-1641.

Eisses, A., 2012, New constraints on slip-rates, recurrence intervals, and strain partitioning beneath Pyramid Lake, Nevada: Master's thesis, University of Nevada, Reno.

Faulds, J. E., and C. D. Henry, 2008, Tectonic influences on the spatial and temporal evolution of the walker lane: An incipient transform fault along the evolving Pacific-North American plate boundary, in Ores and Orogenesis: Circum-Pacific tectonics, geologic evolution, and ore deposits: Arizona Geological Society Digest, 22, 437-470.

Faulds, J. E., C. D. Henry, and N. H. Hinz, 2005, Kinematics of the northern Walker Lane: An incipient transform fault along the Pacific-North American plate boundary: Geological Society of America, 33, 505-508.

Faulds, J. E., and M. E. Perkins, 2007, Evidence for dextral shear along the western margin of the Carson Sink; the missing link between the central and northern Walker Lane, western Nevada: Abstracts with Programs, Geological Society of America, 15-15.

Gundy, T. V., G. Oppliger, M. Ohren, D. Benoit, and M. Morrisson, 2010, Utilizing a comprehensive 3d model to understand, maintain, and expand the Soda Lake geothermal resource, Nevada USA: Transactions, Geothermal Resources Council, 1185-1189.

Gürbüz, A., 2010, Geometric characteristics of pull-apart basins: Lithosphere, 2, 199-206.

Hammond, W. C., G. Blewitt, and C. Kreemer, 2011, Block modeling of crustal deformation of the northern Walker Lane and Basin and Range from gps velocities: Journal of Geophysical Research, 116, 1-28.

Hammond, W. C., C. Kreemer, and G. Blewitt, 2009, Geodetic constraints on contemporary deformation in the northern Walker Lane: 3. Central Nevada seismic belt postseismic relaxation, in Late Cenozoic Structure and Evolution of the Great Basin-Sierra Nevada Transition: Spec. Pap. Geol. Soc. Am., 447, 21.

Hill, D. G., E. Layman, C. M. Swift, and S. H. Yungul, 1979, Soda Lake, Nevada, thermal anomaly: Presented at the Transactions, Geothermal Resources Council.

Koehler, R. D., and S. G. Wesnousky, 2011, Late Pleistocene regional extension rate derived from earthquake geology of late Quaternary faults across the Great Basin, Nevada, between 38.5 n and 40 n latitude: GSA Bulletin, 123, 631-650.

Larsen, P. H., 1988, Relay structures in a lower Permian basement-involved extensional system, east Greenland: Journal of Structural Geology, 10, 3-8.

Mann, P., M. R. Hempton, D. C. Bradley, and K. Burke, 1983, Development of pull-apart basins: Journal of Geology, 91, 529-554.

Maurer, D. K., and A. H. Welch, 2001, Hydrogeology and geochemistry of the Fallon basalt and adjacent aquifers, and potential sources of basalt recharge, in Churchill County, Nevada: Water-Resources Investigations Report 01-4130, U.S. Geological Survey.

McLachlan, H. S., W. R. Benoit, and J. E. Faulds, 2011, Structural framework of the Soda Lake geothermal area, Churchill County, Nevada: Transactions, Geothermal Resources Council, 925-930.

McLachlan, H. S., and J. E. Faulds, 2012, Some new constraints on the stratigraphic and structural setting of the Soda Lake geothermal field, Churchill County, Nevada: Presented at the American Geophysical Union Transactions.

McNitt, J. R., 1990, Stratigraphic and structural controls of the occurrence of thermal fluid at the Soda Lake geothermal field, Nevada: Geothermal Resources Council Transactions, 14.

Reheis, M., 1999, Highest pluvial-lake shorelines and Pleistocene climate of the western Great Basin: Quaternary Research, 52, 196-205.

Sawyer, T.L., c., 1999, Fault number 1679, Rainbow Mountain fault zone,: in Quaternary fault and fold database of the United States: U.S. Geological Survey website, http://earthquakes.usgs.gov/hazards/qfaults, accessed 02/25/2013 10:45 AM.

Sibbett, B. S., 1979, Geology of the Soda Lake geothermal area: Master's thesis, University of Utah Research Institute.

Unruh, J., J. Humphrey, and A. Barron, 2003, Transtensional model for the Sierra Nevada frontal fault system, eastern California: Geology, 31, 327-330.

U.S.G.S., 2006, Quaternary fault and fold database for the United States: from USGS web site: http//earthquakes.usgs.gov/regional/qfaults/, accessed 02/25/2013 10:45 AM.

Wernicke, B., 1992, Cenozoic extensional tectonics of the U.S. Cordillera, in The Cordilleran orogen: Conterminous U.S.: Boulder, Colorado, Geological Society of America, Geology of North America, G-3, 553-581.

Wesnousky, S. G., 2005a, Active faulting in the Walker Lane: Tectonics, 24, 1-35.

Wesnousky, S.G., 2005b, The San Andreas and Walker Lane fault systems, western North America: transpression, transtension, cumulative slip and the structural evolution of a major transform plate boundary: Journal of Structural Geology, 27, 1505-1512.

Wesnousky, S. G., J. M. Bormann, C. Kreemer, W. C. Hammond, and J. N. Brune, 2012, Neotectonics, geodesy, and seismic hazard in the northern Walker Lane of western North America: Thirty kilometers of crustal shear and no strike-slip?: Earth and Planetary Science Letters, 329, 133-140.

Wu, J. E., K. McClay, P. Whitehouse, and T. Dooley, 2009, 4d analogue modelling of transtensional pull-apart basins: Marine and Petroleum Geology, 26, 1608-1623.

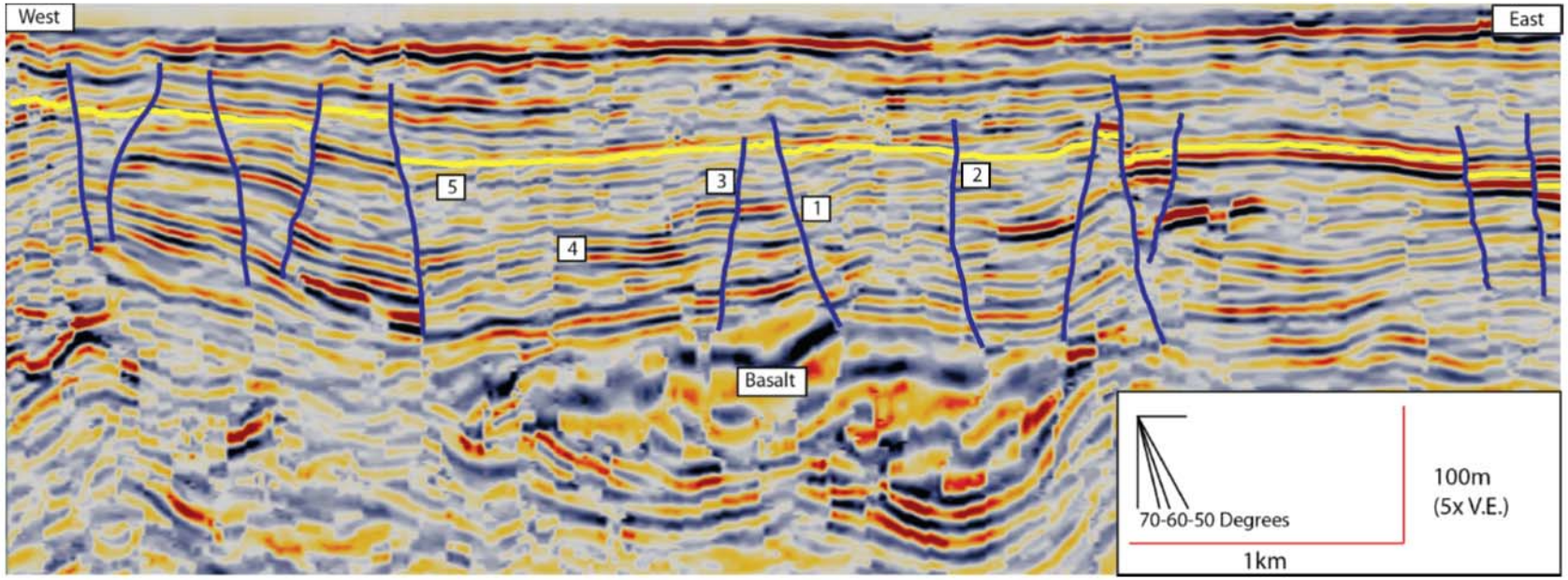

Figure 4: This fault-enhanced inline vertical section demonstrates the variety of the fault picks with horst and graben features across the study. The 5.1 Ma basaltic unit is indicated by the high amplitude and long wavelength reflections.